

§6 Mathematical Background of FRDC Method

6. 1 Introduction

While the ac-dc transfer difference is defined using sinusoidal waveform, the FRDC-DC difference is defined using rectangular waveforms. The comparison of the frequency characteristics between the ac-dc difference and the FRDC-DC difference is discussed in section 6.2.1. A formula which represents the frequency characteristic of the FRDC-DC difference is derived in section 6.2.2, using a simple exponential behavior for the thermoelectric effects. Physical significance of the thermoelectric time-constant is discussed in section 6.2.3.

As described in section 4.1, the higher-order components of the FRDC waveform may be filtered by frequency characteristic of the input circuit, and may affect the equality in the rms-values for FRDC- and dc-modes. The effects of the higher-order components are evaluated in section 6.3, using a simple circuit-model for the input circuit of the TVCs.

6. 2 Thermoelectric effect in TC

6. 2. 1 Thermoelectric effect and FRDC-DC difference

The ac-dc transfer difference is determined by the difference between the EMF outputs of a thermal converter for steady-state dc and for a sinusoidal waveform of the same rms amplitude, as defined by equation (1.5) in section 1.2.

$$\delta_{AC-DC} \cong -\frac{E_{AC} - E_{DC}}{nE_{DC}} \quad (1.5)$$

Similarly, the FRDC-DC difference δ_{FRDC} is determined by the difference between the EMF outputs for the FRDC- and the dc-modes as,

$$\delta_{FRDC-DC} \cong -\frac{E_{FRDC} - E_{DC}}{nE_{DC}} \quad (1.8)$$

In the case of modified waveform, the quantities E_{FRDC} and E_{DC} represent the average EMFs for the two MDR modes and for the two CPDC modes respectively, as defined by,

$$\begin{aligned} E_{FRDC} &\equiv \frac{E_{MDFR(1)} + E_{MDFR(2)}}{2} \\ E_{DC} &\equiv \frac{E_{CPDC+} + E_{CPDC-}}{2} \end{aligned} \quad (6.1)$$

As discussed in section 1.2.3, the ac-dc transfer difference of a thermal converter is caused by the following three independent effects;

(a) Low-frequency effect δ_{LF} due to thermal ripple at the heater.

(b) High-frequency effect δ_{HF} due to frequency characteristic of input circuit.

(c) Thermoelectric transfer difference δ_{TE} due to Thomson and Peltier effects.

When a steady-state dc is applied to a thermal converter, the thermoelectric effects appears at the output EMF E_{DC} as,

$$\begin{cases} E_{DC+} = E_{joule}^{DC} + \Delta E_{TE(1st)}^{DC} + \Delta E_{TE(2nd)}^{DC} \\ E_{DC-} = E_{joule}^{DC} - \Delta E_{TE(1st)}^{DC} + \Delta E_{TE(2nd)}^{DC} \end{cases} \quad (6.2)$$

The first term E_{joule}^{DC} represents the joule heating for the steady-state dc, and the other terms $\Delta E_{TE(1st)}^{DC}$ and $\Delta E_{TE(2nd)}^{DC}$ represents the first-order and the second-order thermoelectric effects. The first-order effects $\Delta E_{TE(1st)}^{DC}$ are compensated by taking the mean of the output EMFs, E_{DC+} and E_{DC-} .

When a sinusoidal-waveform input signal is applied to a thermal converter, the output EMF E_{AC} is described as,

$$E_{AC} \equiv E_{joule}^{SIN}(f) + \Delta E_{HF}^{SIN}(f) + \Delta E_{TE(2nd)}^{SIN}(f), \quad (6.3)$$

where $E_{joule}^{SIN}(f)$ represents the joule heating for the rms power of the sinusoidal waveform. At the low-frequency range ($f < 100\text{Hz}$), it deviates from its dc-counterpart E_{joule}^{DC} causing the low-frequency effect δ_{LF} in the ac-dc transfer difference. The change in the EMF $E_{HF}^{SIN}(f)$ due to high-frequency effect is significant in the frequency range above 10 kHz.

Combining (6.2), (6.3) with (1.6), the ac-dc difference of a thermal converter is represented as,

$$\begin{aligned} \delta_{AC-DC} &\cong -\frac{1}{nE_{DC}} \left\{ [E_{joule}^{SIN}(f) - E_{joule}^{DC}] + \right. \\ &\quad \left. + \Delta E_{HF}^{SIN}(f) + [\Delta E_{TE(2nd)}^{SIN}(f) - \Delta E_{TE(2nd)}^{DC}] \right\} \\ &= \delta_{LF}(f) + \delta_{HF}(f) + \delta_{TE} - \delta_{TE}^{SIN}(f). \end{aligned} \quad (6.4)$$

The term $\delta_{TE}^{SIN}(f)$ represents the thermoelectric effect for sinusoidal waveform which exist only at very low frequencies ($f \ll 100\text{Hz}$). Since the thermoelectric effect is much smaller than the low-frequency effect δ_{LF} , the equation may be simplified as,

$$\delta_{AC-DC} \cong \delta_{LF}(f) + \delta_{HF}(f) + \delta_{TE}. \quad (6.5)$$

A typical frequency characteristic of the ac-dc difference represented by the (6.5) has been illustrated in Figure 1.6.

In the FRDC-DC difference measurement, the output EMFs E_{CPDC} for CPDC waveforms are described as,

$$\begin{cases} E_{CPDC+} = E_{joule}^{CPDC}(f_{SW}) + \Delta E_{HF}^{CPDC}(f_{SW}) + \Delta E_{TE(1st)}^{CPDC} + \Delta E_{TE(2nd)}^{CPDC} \\ E_{CPDC-} = E_{joule}^{CPDC}(f_{SW}) + \Delta E_{HF}^{CPDC}(f_{SW}) - \Delta E_{TE(1st)}^{CPDC} + \Delta E_{TE(2nd)}^{CPDC}. \end{cases} \quad (6.6)$$

The first term E_{joule}^{CPDC} represents the joule heating for the rms power of the CPDC waveform. The high-frequency components of CPDC waveform give rise to the error term $\Delta E_{HF}^{CPDC}(f_{SW})$ which contributes an error term $\delta_{HF}^{CPDC}(f_{SW})$ to the FRDC-DC difference. The terms $\Delta E_{TE(1st)}^{CPDC}$ and $\Delta E_{TE(2nd)}^{CPDC}$ represent the first-order and the second-order thermoelectric effects in CPDC waveform.

The output EMF E_{FRDC} for MDFR waveform is described as,

$$E_{FRDC} \cong E_{joule}^{MDFR}(f_{SW}) + \Delta E_{HF}^{MDFR}(f_{SW}) + \Delta E_{TE(2nd)}^{MDFR}(f_{SW}). \quad (6.7)$$

The joule heating in MDFR waveform produces the EMF output $E_{joule}^{MDFR}(f_{SW})$ which is exactly equal to $E_{joule}^{CPDC}(f_{SW})$. Furthermore, if the off-time t_{off} is much smaller than the time constant of joule heating ($t_{off} \ll t_{joule}$), the thermal ripple is not created even at frequencies near dc.

Combining (1.7), (6.6) and (6.7), the FRDC-DC difference of a thermal converter is described as,

$$\begin{aligned} \delta_{FRDC-DC} &\cong -\frac{1}{nE_{DC}} \left\{ [\Delta E_{HF}^{MDFR}(f_{SW}) - \Delta E_{HF}^{CPDC}(f_{SW})] \right. \\ &\quad \left. + [\Delta E_{TE(2nd)}^{MDFR}(f_{SW}) - \Delta E_{TE(2nd)}^{CPDC}(f_{SW})] \right\} \\ &\cong \delta'_{HF}(f_{SW}) + \delta_{TE} - \delta_{TE}^{FRDC}(f_{SW}). \end{aligned} \quad (6.8)$$

The first term $\delta'_{HF}(f_{SW})$ represents high-frequency characteristic of FRDC-DC difference of a thermal converter. Since the terms $\Delta E_{HF}^{MDFR}(f_{SW})$ and $\Delta E_{HF}^{CPDC}(f_{SW})$ tend to cancel out, as will be described in section 6.3, the term $\delta'_{HF}(f_{SW})$ does not give significant contribution up to 10 kHz.

The second term δ_{TE} and the third term $\delta_{TE}^{FRDC}(f_{SW})$ correspond to the thermoelectric effects $\Delta E_{TE(2nd)}^{CPDC}$ and $\Delta E_{TE(2nd)}^{MDFR}(f_{SW})$, in the limit $t_{off} \rightarrow 0$. The effect of the off-time on the FRDC-DC difference measurement is negligible as long as the off-time is much shorter than the switching period ($t_{off} \ll T_{SW}$). The quantitative analysis on the effect of off-time is given in the Appendix(B).

In the case of ac-dc difference, frequency dependence of the thermoelectric effect $\delta_{TE}^{SIN}(f)$ can not be observed because the effect is masked by much larger effect from the thermal ripple $\delta_{LF}(f)$ due to sinusoidal joule heating. On

the other hand, no thermal ripple is produced by the rectangular FRDC waveform, and the low-frequency characteristic is dominated by the thermoelectric effects $\delta_{TE}^{FRDC}(f_{SW})$. Thus, by performing a FRDC-DC difference measurement at lower frequencies, a thermoelectric time constant τ_{TE} of a TC may be estimated from low-frequency characteristics.

It is possible to choose the switching frequency f_{SW} such that the following two conditions are satisfied:

(a) The switching frequency f_{SW} is sufficiently higher than the inverse of the thermoelectric time constant τ_{TE} .

(b) The switching frequency f_{SW} is sufficiently lower than a characteristic frequency f_{HF} above which the effect of high-frequency components becomes significant. In this case, setting $\delta_{TE}^{FRDC}(f_{SW}) \ll \delta_{TE}$ and $\delta'_{HF}(f_{SW}) \ll \delta_{TE}$, we obtain

$$\delta_{FRDC-DC} (1/\tau_{TE} \ll f_{SW} \ll f_{HF}) \cong \delta_{TE}. \quad (6.9)$$

Since the thermoelectric transfer difference of a thermal converter can be evaluated by the FRDC-DC difference measurement, the FRDC method may be regarded as an independent basis for ac-dc transfer standard.

The estimation of the thermoelectric time constant τ_{TE} will be described in detail in the next sub-section. The effect of high-frequency components $\delta'_{HF}(f_{SW})$ will be analyzed using a fouler analysis in section 6.3.

6. 2. 2 Frequency response of thermoelectric effect

The frequency dependence of the FRDC-DC difference at lower frequencies is characterized by the thermoelectric effects. A simple mathematical model of the thermoelectric effect in a thermal converter is given by **figure 6.1**(a). In this

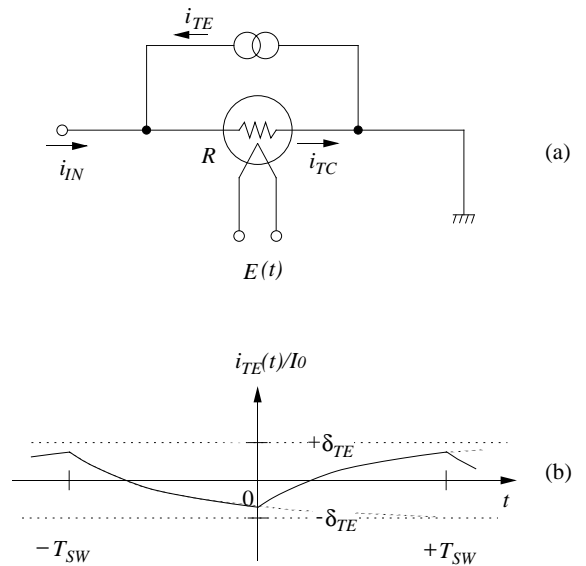


Figure 6.1 (a) Mathematical model which represents the thermoelectric effect in the thermal converter. The thermoelectric effect is represented by an imaginary current source which produces an excess current i_{TE} (b) The exponential behavior of the excess current i_{TE} for a rectangular input waveform.

model, the thermoelectric effect is represented by an additional current $i_{TE}(t)$ which is described by:

$$i_{TE}(t) = I_0 \delta_{TE} \left(1 - e^{-(t-\Delta t)/\tau_{TE}}\right) \quad (\text{for } 0 \leq t < T_{SW}). \quad (6.10)$$

In the steady-state condition ($i_{IN} = i_0$), the excess current $i_{TE} = \delta_{TE} i_0$ causes the thermoelectric transfer difference δ_{TE} . When the input current $i_{IN}(t)$ is reversed with a switching period T_{SW} , the excess current $i_{TE}(t)$ responds exponentially with a time-constant τ_{TE} as shown in Figure 6.1(b).

At the reversal of the input current, the excess current $i_{TE}(t)$ must satisfy the following boundary condition;

$$i_{TE}(T_{SW}) = i_{TE}(0). \quad (6.11)$$

where T_{SW} is the switching period for reversing the input current. Combining the condition (6.11) with (6.10), we obtain

$$\Delta t = \tau_{TE} \log\left(\frac{2}{1 + e^{-T_{SW}/\tau_{TE}}}\right). \quad (6.12)$$

Then, the effective power P which is dissipated at the heater of the thermal converter is given as,

$$\begin{aligned} P &\equiv \frac{1}{2} R \langle i_{TC}(t) \rangle_{\text{rms}}^2 = \frac{1}{2} R \left[\frac{1}{T_{SW}} \int_0^{T_{SW}} \{i_{TC}(t)\}^2 dt \right] \\ &= \frac{1}{2} R I_0^2 \left[\frac{1}{T_{SW}} \int_0^{T_{SW}} \left\{1 + \delta_{TE} \left(1 - e^{-(t-\Delta t)/\tau_{TE}}\right)\right\}^2 dt \right]. \end{aligned} \quad (6.13)$$

Since $\delta_{TE} \ll 1$, we can expand (6.13) to the first order of δ_{TE} . Neglecting the second and the higher order terms, we obtain;

$$\begin{aligned} P &\cong \frac{1}{2} R I_0^2 \left[\frac{1}{T_{SW}} \int_0^{T_{SW}} \left\{1 + 2\delta_{TE} \left(1 - e^{-(t-\Delta t)/\tau_{TE}}\right)\right\} dt \right] \\ &= \frac{1}{2} R I_0^2 \left[1 + 2\delta_{TE} \left\{1 - \left(\frac{2\tau_{TE}}{T_{SW}}\right) \tanh\left(\frac{T_{SW}}{2\tau_{TE}}\right)\right\} \right]. \end{aligned} \quad (6.14)$$

Assuming that the output EMF is proportional to the input power P , the FRDC-DC difference is calculated as

$$\delta_{FRDC-DC} = \delta_{TE} \left(\frac{2\tau_{TE}}{T_{SW}}\right) \tanh\left(\frac{T_{SW}}{2\tau_{TE}}\right). \quad (6.15)$$

The period T_{SW} is the inverse of the reversing frequency and one-half of the inverse of basic frequency.

The frequency dependence of the derived formula (6.15) is shown in **figure 6.2**. If the switching period is sufficiently longer than the thermoelectric time constant, $f_{SW} \ll (1/\tau_{TE})$, then the FRDC-DC difference approaches to zero. This is because the slow-reversing waveform produces the same temperature distribution as in the case of steady-state dc. On the other hand, if the switching period is sufficiently shorter than

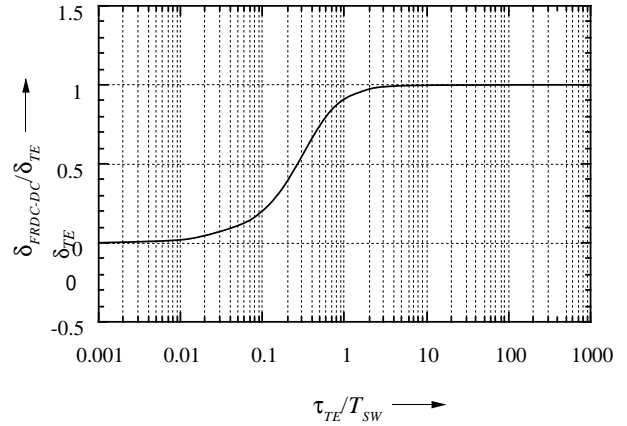


Figure 6.2 The estimated frequency characteristic of the FRDC-DC difference of a thermal converter due to thermoelectric effect. At sufficiently high switching frequency $f_{SW} \gg (1/\tau_{TE})$, the FRDC-DC difference equals to the thermoelectric transfer difference δ_{TE} .

the thermoelectric time constant, $f_{SW} \gg (1/\tau_{TE})$, then the thermoelectric effect is not developed in the FRDC mode, and the FRDC-DC difference equals the thermoelectric transfer difference δ_{TE} .

In the case of SJTCs, the parameters δ_{TE} and τ_{TE} are of the order of 0.01 s to 1s and 10^{-6} to 10^{-5} , respectively. The two parameters can be calculated by the least-square fitting of measured data to the formula (6.15). Some types of SJTC show more complex frequency characteristics, requiring two or three different time-constants τ_{TE} to be fitted by the theoretical curve properly.

In this section we did not take the off-time into account, because the off-time is less than 0.1 % of the switching period at lower frequency (<100 Hz). The more exact derivation of the (6.15) taking the effect of off-time will be given in the Appendix B.

6. 2. 3 Time constants of SJTC

Since the speed of heat-transfer is finite, there is a relationship between the characteristic size and the characteristic time constant of a thermal system. In the case of a one-dimensional uniform heater, the heat-transfer is characterized by the following differential equation.

$$\frac{\partial \theta}{\partial t} = \frac{k}{C_v} \frac{\partial^2 \theta}{\partial x^2} \quad (6.16)$$

When heat-impulse is applied at the point $x=0$ and at the time $t=0$, the normalized temperature distribution $f(x,t)$ is given by a Gauss distribution function:

$$f(x,t) = \frac{1}{\sqrt{4\pi a t}} e^{-x^2/4a^2 t} \quad (6.17)$$

which is called ‘‘point-source’’ solution of the heat-transfer equation. The width λ_1 of the Gauss distribution after the

time-interval τ is defined by

$$f(\pm\lambda_1, \tau) = e^{-1} f(0, \tau), \quad (6.18)$$

and is calculated as

$$\lambda_1 = 2a\sqrt{\tau} = \sqrt{4k\tau/C_V}. \quad (6.19)$$

The width λ_1 is a measure for the spread of the heat during the time interval τ . In other words, if a one-dimensional thermal system exhibits a characteristic time constant τ , the characteristic scale of the system is estimated to be of the order of λ_1 .

When the heat is generated continuously at point $x=0$, the temperature distribution is proportional to $g(x, t)$ which is obtained by integrating the point-source solution (6.17).

$$g(x, t) = \int_0^t \frac{1}{\sqrt{4\pi at}} e^{-x^2/4a^2t} dt \quad (6.20)$$

In the case of a continuous heating, the distribution function satisfies the following relation for arbitrary constant β :

$$g(\beta x, \beta^2 t) = \beta g(x, t). \quad (6.21)$$

The distribution function $g(x, t)$ conserves its shape with time. The width of the distribution λ_2 for continuous heating is defined by a condition similar to (6.18);

$$\lambda_2 = \frac{2a\sqrt{\tau}}{\xi_0} = \frac{\sqrt{4k\tau/C_V}}{\xi_0}. \quad (6.22)$$

Here the constant $\xi_0 = 2.06$ is a non-dimensional constant determined by;

$$\int_0^{\xi_0} \frac{1}{\sqrt{\xi}} (e^{-1/\xi} - e^{-1}) d\xi = 0. \quad (6.23)$$

By the use of the formula (6.19) and (6.22), the characteristic scale of the thermoelectric effects is evaluated from the time-constant τ_{TE} , which is determined by the frequency dependence of the FRDC-DC difference measurement. In both of the cases, the widths λ_1 and λ_2 are proportional to the square-root of the time-interval τ .

6.3 Effect of higher-order components

The rectangular FRDC-waveform contains a large number of harmonics, and the higher-order components may be filtered by shunt capacitance or the dielectric loss in the input circuit. As discussed in section 4.2.2, the rms power of the n -th order components decreases as $1/n^2$ with the frequency, while the loss of power for each component increases as n^2 . As a result, even at reversing frequency as low as 100 Hz, more than 0.1 ppm of the power will be lost for the FRDC-modes.

In the case of modified waveform, not only the FRDC

(MDFR) modes but also the dc (CPDC) modes have the higher order components. Since the CPDC waveform includes the same number of up-going and down-going steps as the MDFR waveform, they have similar power spectrum for the high-frequency components. In this case, the power-loss in the FRDC-modes are mostly compensated by the CPDC-modes, and a large reduction of the effect due to the higher-order components is expected.

In this section, power spectrum for the high-frequency components for the MDFR modes and the CPDC modes are calculated. Then the effect of the higher-order components to the FRDC-DC difference measurement is evaluated using simplified circuit models for the input circuit of the thermal converters.

6.3.1 Fourier components of FRDC waveform

The waveform of the input voltage $e_{IN}(t)$ may be expanded in the complex Fourier series:

$$e_{IN}(t) = \sum_{n=-\infty}^{+\infty} \alpha_n e^{in2\pi f_0 t}, \quad (6.24)$$

where the base frequency f_0 is defined by the switching frequency of analog switches f_{SW} :

$$f_0 \equiv f_{SW}/2 = 1/(2T_{SW}). \quad (6.25)$$

The period T_{SW} is the inverse of the switching frequency f_{SW} and one-half of the inverse of base frequency. The original FRDC waveform are represented by the normalized functions $f(t)$ and $g(t)$ as,

$$\begin{aligned} f(t) &\equiv [e_{IN}(t)]_{DC}/e_0 = 1 \\ g(t) &\equiv [e_{IN}(t)]_{FRDC}/e_0 = \sum_{\substack{n=-\infty \\ n=odd}}^{+\infty} \frac{2}{in\pi} e^{in2\pi f_0 t}, \end{aligned} \quad (6.26)$$

where e_0 is the amplitude of the CPDC- and MDFR-wave-

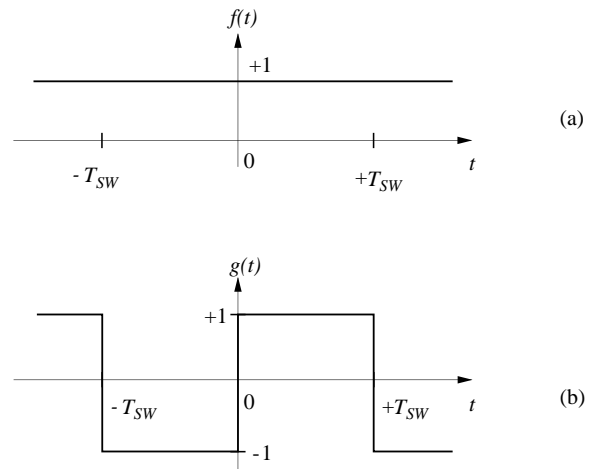


Figure 6.3 Normalized waveforms $f(t)$ and $g(t)$ for the original FRDC with switching-frequency f_{SW} . The function $g(t)$ has higher harmonics for the odd-numbers of n .

form. The function $f(t)$ represents for the dc mode and the function $g(t)$ represents the FRDC mode, as shown in **figure 6.3**. The function $g(t)$ has higher harmonics for the odd-numbers of n .

The ‘glitch’ or the ‘off-time’ introduced in the modified waveform can be represented by the functions $u(t)$ and $v(t)$, as shown in **figure 6.4**. These functions have train of spikes of width t_{off} . The waveform for the CPDC mode and thMDF mode are derived by the combinations $f(t)+u(t)$ and $g(t)+v(t)$, respectively. The Fourier components of waveforms $u(t)$ and $v(t)$ is readily obtained as

$$\begin{aligned} u(t) &= \sum_{\substack{n=-\infty \\ n=even}}^{+\infty} \frac{-1}{in\pi} (1 - e^{-in\pi\epsilon}) e^{in2\pi f_0 t} \\ &= \sum_{\substack{n=-\infty \\ n=even}}^{+\infty} \frac{2}{n\pi} \sin\left(\frac{n\pi\epsilon}{2}\right) e^{in2\pi f_0 (t-t_{off}/2)} \\ v(t) &= \sum_{\substack{n=-\infty \\ n=odd}}^{+\infty} \frac{-1}{in\pi} (1 - e^{-in\pi\epsilon}) e^{in2\pi f_0 t} \\ &= \sum_{\substack{n=-\infty \\ n=odd}}^{+\infty} \frac{2}{n\pi} \sin\left(\frac{n\pi\epsilon}{2}\right) e^{in2\pi f_0 (t-t_{off}/2)} \end{aligned} \quad (6.27)$$

Here, the ‘duty ratio’ ϵ is defined by,

$$\epsilon = 2f_0 t_{off} = f_{sw} t_{off} = t_{off} / T_{sw}. \quad (6.28)$$

Combining (6.26) and (6.27), the Fourier components of the waveform for CPDC mode are given by,

$$\begin{aligned} [e_{IN}(t)/e_0]_{CPDC} &= f(t) + u(t) \\ &= 1 - \sum_{\substack{n=-\infty \\ n=even}}^{+\infty} \frac{2}{n\pi} \sin\left(\frac{n\pi\epsilon}{2}\right) e^{in2\pi f_0 (t-t_{off}/2)}. \end{aligned} \quad (6.29)$$

Similarly, the Fourier components of the waveform for MDFR mode are given by,

$$\begin{aligned} [e_{IN}(t)/e_0]_{MDFR} &= g(t) + v(t) \\ &= \sum_{\substack{n=-\infty \\ n=odd}}^{+\infty} \frac{1}{in\pi} (1 + e^{-in\pi\epsilon}) e^{in2\pi f_0 t} \\ &= \sum_{\substack{n=-\infty \\ n=odd}}^{+\infty} \frac{2}{in\pi} \cos\left(\frac{n\pi\epsilon}{2}\right) e^{in2\pi f_0 (t-t_{off}/2)}. \end{aligned} \quad (6.30)$$

When $t_{off} \rightarrow 0$, all the components (except for the 0th-order component) of the CPDC-waveform reduce to zero. In this case, the components of MDFR-waveform approach to that of the original FRDC. The Fourier components of the FRDC, CPDC and MDFR modes are summarized in **table 6.1**.

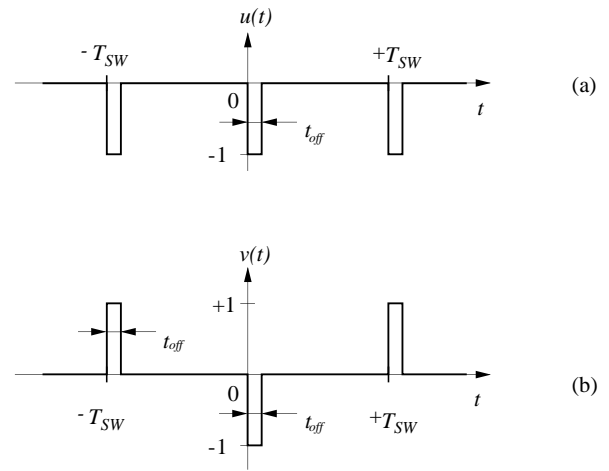


Figure 6.4 Functions $u(t)$ and $v(t)$, which represent train of spikes of width t_{off} with switching-frequency f_{sw} . The combined functions $f(t)+u(t)$ and $g(t)+v(t)$ represent the waveforms for the ‘chopped’ dc (CPDC) mode and modified FRDC (MDFR) mode, respectively.

Table 6.1 The calculated harmonics for original waveforms [$f(t)$, $g(t)$], the train of spikes [$u(t)$, $v(t)$], and modified waveforms [$f(t)+u(t)$, $g(t)+v(t)$].

	α_n	$ \alpha_n (\text{odd})$	$ \alpha_n (\text{even})$
$f(t)$	1	0	0
$g(t)$	0	$\frac{2}{n\pi}$	0
$u(t)$	$-\epsilon$	0	$\frac{2}{n\pi} \sin\left(\frac{n\pi\epsilon}{2}\right)$
$v(t)$	0	$\frac{2}{n\pi} \sin\left(\frac{n\pi\epsilon}{2}\right)$	0
$f(t)+u(t)$	$1-\epsilon$	0	$\frac{2}{n\pi} \sin\left(\frac{n\pi\epsilon}{2}\right)$
$g(t)+v(t)$	0	$\frac{2}{n\pi} \cos\left(\frac{n\pi\epsilon}{2}\right)$	0

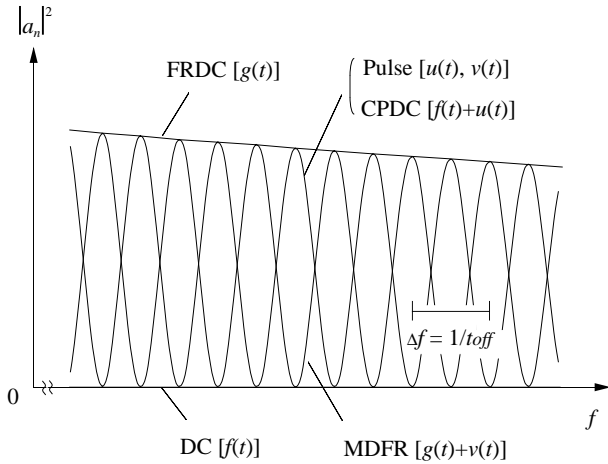


Figure 6.5 The frequency characteristics of the power spectrum of FRDC, CPDC and MDFR modes. The functions $u(t)$ and $v(t)$ are represented by a periodic envelope which oscillates between $(2/n\pi)$ and 0 with a period $\Delta f = 1/t_{off}$. The original FRDC waveform $g(t)$ is characterized by an envelope $(2/n\pi)$.

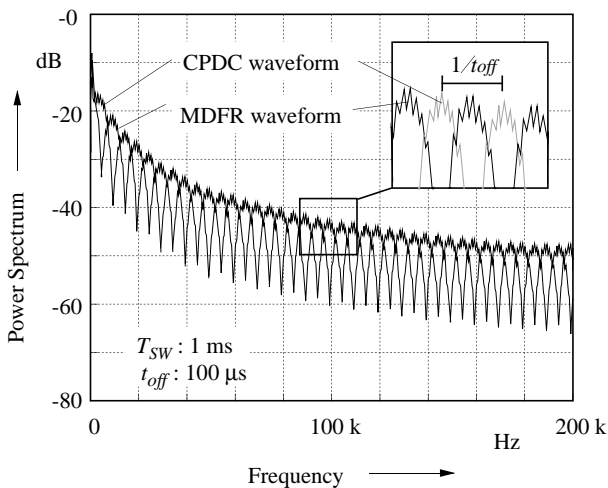


Figure 6.6 The Fourier components for the CPDC and MDFR waveforms measured by a spectrum analyzer for the parameter of $t_{off} = 100 \mu s$ and $f_{sw} = 1 ms$.

The frequency characteristics of the power spectrum of FRDC, CPDC and MDFR modes are illustrated in **figure 6.5**. The functions $u(t)$ and $v(t)$ are represented by a periodic envelope which oscillates between $(2/n\pi)$ and 0 with a period $\Delta f = 1/t_{off}$. The original FRDC waveform $g(t)$ is characterized by an envelope $(2/n\pi)$. The steady-state dc obviously has no Fourier components. Hence the difference between $(2/n\pi)$ and 0 gives a measure for the high-frequency effect in the original FRDC-DC measurement.

The waveform for CPDC has a periodic envelope which oscillates between $(2/n\pi)$ and 0 with a period $\Delta f = 1/t_{off}$. Since $f(t)$ has no Fourier components, the waveform for CPDC $[f(t)+u(t)]$ has the same periodic envelope as $u(t)$. In the case of MDFR-waveform, Fourier components of $g(t)$ are partly compensated by the component of $v(t)$, and the waveform $[g(t)+v(t)]$ has similar periodic envelope with a phase shifted

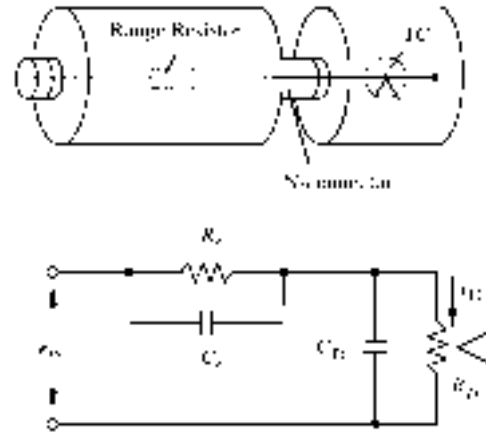


Figure 6.7 The equivalent circuit diagram of the TC-Range resistor combination. The capacitance C_{TC} shunts the heater resistance R_{TC} and C_r shunts the current-limiting resistor R_c .

180 degree $(\Delta f/2)$ relative to that of CPDC.

The Fourier components for the CPDC and MDFR waveforms were experimentally confirmed by use of a spectrum analyzer for the parameter of $t_{off} = 100 \mu s$ and $f_{sw} = 1 ms$, as shown in **figure 6.6**. Since the difference of the power spectrum between CPDC and MDFR is much smaller than the difference between the original FRDC and steady-state dc, a large reduction of the effect from the higher-order components is expected for the modified waveform.

6.3.2 Frequency characteristic of TC-input circuit

The effect of shunt capacitance may become significant when thermal converters are connected in series with current-limiting resistors ('range resistors'), and measured with the voltage mode. The equivalent input circuit diagram for this set-up is shown in **figure 6.7**[37]. The heater resistance (R_{TC}) is normally around 25Ω for a 10 mA-type SJTC. The shunt capacitance C_{TC} is mainly due to the capacitance of type-N connector inserted between the range-resistor and the thermal converter, and is of the order of a few pF. In the case of 10 V measurement, a $1k\Omega$ metal-film resistor is used as a range-resistor (R_r) which limits the heater current to 10 mA. The metal-film resistor has a shunt capacitance (C_r) of about a few tenths of a pF, which exists between the two leads of the resistor.

When the voltage $e_{IN}(t)$ is applied at the input of the thermal converter, current $i_{TC}(t)$ which passes through the heater of thermal converter may be expressed as

$$i_{TC}(t) \equiv \sum_{n=-\infty}^{+\infty} \beta_n e^{in2\pi f_0 t} = \sum_{n=-\infty}^{+\infty} \alpha_n Y_n e^{in2\pi f_0 t} \quad (6.31)$$

The conductance Y_n is readily calculated for the equivalent input circuit:

$$\begin{aligned}
 Y_n &\equiv \beta_n / \alpha_n \\
 &= \frac{1}{R_r + R_{tc}} \times \frac{1 + 2i\pi C_r R_r n f_0}{1 + 2i\pi C_p R_p n f_0} = \frac{1 + 2i\pi \tau_r n f_0}{1 + 2i\pi \tau_p n f_0} Y_0
 \end{aligned} \quad (6.32)$$

where the nominal conductance (Y_0), the characteristic time constants (τ_p , τ_r), and ‘parallel’ capacitance and resistance (C_p , R_p) are defined by,

$$\begin{cases} Y_0 \equiv 1/(R_r + R_{tc}) \\ \tau_p \equiv C_p R_p, \quad \tau_r \equiv C_r R_r \\ C_p \equiv C_r + C_{tc}, \quad 1/R_p \equiv 1/R_r + 1/R_{tc}. \end{cases} \quad (6.33)$$

Then, the effective power P which is dissipated at the heater of the thermal converter is

$$\begin{aligned}
 P &\equiv \frac{1}{2} R_{tc} \langle i_{tc}(t) \rangle_{\text{rms}}^2 = \frac{1}{2} R_{tc} \left[\frac{1}{T} \int_0^T \{i_{tc}(t)\}^2 dt \right] \\
 &= \frac{1}{2} R_{tc} \sum_{n=-\infty}^{+\infty} |\beta_n|^2 = P_0 \sum_{n=-\infty}^{+\infty} |\alpha_n / e_0|^2 |Y_n / Y_0|^2
 \end{aligned} \quad (6.34)$$

where the nominal power P_0 is defined by,

$$P_0 \equiv \frac{1}{2} R_{tc} e_0^2 Y_0^2 = \frac{R_{tc}}{2(R_r + R_{tc})^2} e_0^2. \quad (6.35)$$

The change in the power-dissipation $\Delta P/P_0$ due to shunt capacitance is

$$\frac{\Delta P}{P_0} \equiv \frac{P - P_0}{P_0} = -1 + \sum_{n=-\infty}^{+\infty} |\alpha_n / e_0|^2 |Y_n / Y_0|^2. \quad (6.36)$$

Combining (6.36) with (6.29) and (6.30), effect of fre-

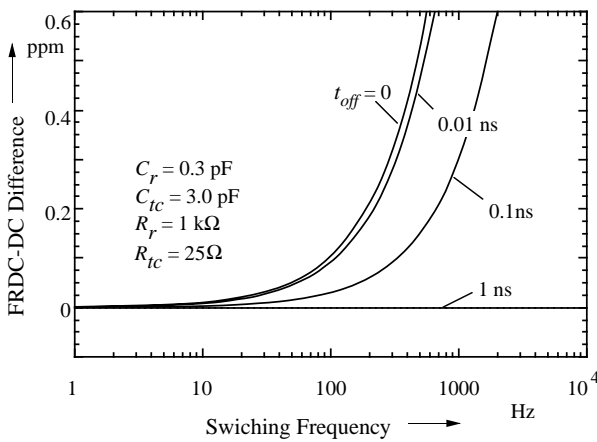


Figure 6.8 The effect of shunt capacitance on the FRDC-DC difference measurement calculated for the typical circuit-parameters $R_r=1000 \Omega$, $R_{TC}=25 \Omega$, $C_r=0.3 \text{ pF}$ and $C_{TC}=3 \text{ pF}$.

quency characteristic of TC-input circuit on the FRDC-DC difference measurement is given by the following formula. [The derivation of (6.37) is described in the Appendix C]

$$\begin{aligned}
 \delta_{FRDC-DC} &= \frac{1}{2} \left\{ \left[\frac{\Delta P}{P_0} \right]_{CPDC} - \left[\frac{\Delta P}{P_0} \right]_{MDFR} \right\} \\
 &= 4\tau_r \left(\frac{\tau_p}{\tau_r} - \frac{\tau_r}{\tau_p} \right) f_0 e^{-t_{off}/\tau_p}.
 \end{aligned} \quad (6.37)$$

For the typical circuit-parameters $R_r=1000 \Omega$, $R_{TC}=25 \Omega$, $C_r=0.3 \text{ pF}$ and $C_{TC}=3 \text{ pF}$, the characteristic time-constants τ_p and τ_r are calculated as $8 \times 10^{-11} \text{ s}$ and $3 \times 10^{-10} \text{ s}$ respectively. The difference of total effective power between CPDC- and MDFR-waveform is calculated from (6.30):

$$\begin{aligned}
 \delta_{FRDC-DC} &\equiv 2.1 \times 10^{-9} f_0 (\text{Hz}) \times e^{-12.5 \times t_{off} (\text{ns})} \\
 &\equiv 1.1 \times 10^{-9} f_{SW} (\text{Hz}) \times e^{-12.5 \times t_{off} (\text{ns})}.
 \end{aligned} \quad (6.38)$$

The obtained frequency dependence is illustrated in **Figure 6.8**. In the case of $t_{off}=0$, which represents for the original FRDC waveform, effect on the FRDC-DC difference is proportional to the reversing frequency, and can be larger than 10^{-7} at the switching frequency of 100 Hz.

While in the case of modified waveform, the effect is suppressed by a factor $\exp(-t_{off}/\tau_p)$. Since the off time t_{off} ($>1 \mu\text{s}$) is sufficiently longer than the characteristic time constant of the input circuit τ_p (0.1 ns), the effect becomes negligible up to 10 kHz. The suppression is due to the interlaced pattern of the power spectrum of the CPDC- and MDFR-waveform, as was shown in Figure 6.5 and 6.6.

6.3.3 Effect of dielectric loss/absorption

In the previous section, the effect of shunt capacitance has been evaluated in the voltage mode. When the TVCs are measured at current mode, the effect of dielectric loss/absorption in the input circuit becomes significant. The equivalent circuit diagram which describes this effect is given in **figure 6.9**. The input capacitance (C_d) and the effective leak-

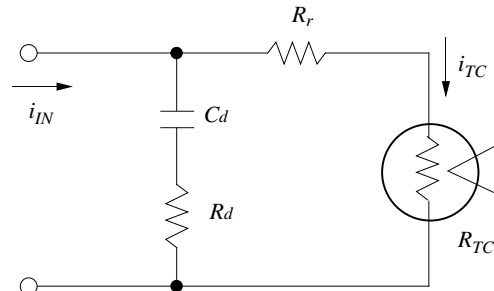


Figure 6.9 The equivalent circuit diagram which represents the effect of dielectric loss in the input circuit. The dielectric loss is represented by the input capacitance C_d and the effective leakage resistance R_d which are of the order of 0.1 pF and 1 GΩ respectively.

age resistance (R_d) are of the order of 0.1 pF and 1 GΩ respectively.

Using the same procedure as in the case of the previous section, the conductance Y_n is calculated from the circuit diagram as,

$$Y_n = \frac{1 + 2i\pi C_{leak} R_{leak} n f_0}{1 + 2i\pi C_{leak} R_{leak} n f_0} = \frac{1 + 2i\pi \tau_{leak} n f_0}{1 + 2i\pi \tau_{leak} n f_0} \quad (6.39)$$

The equation (6.39) has the same functional dependence on the characteristic time constants (τ_{leak} , τ'_{leak}), which are defined by,

$$\tau_{leak} = \frac{C_{leak} R_{leak}}{k \cdot R_r \cdot R_{lc}} \quad (6.40)$$

The influence of the dielectric loss/absorption on the FRDC-DC difference can be estimated by replacing the time constants (τ_p , τ'_p) with (τ_{leak} , τ'_{leak}) in the (6.37).

$$\delta_{FRDC-DC} = \tau_{leak} \left(\frac{\tau'_{leak}}{\tau_{leak}} - \frac{\tau_{leak}}{\tau'_{leak}} \right) f_0 e^{-t_{off}/\tau_{leak}} \quad (6.41)$$

For the typical circuit-parameters for a TVC, $R_r=1000\Omega$, $R_{lc}=25\Omega$, the two time constants are calculated as $\tau_{leak} \approx \tau'_{leak} \approx 1 \times 10^{-4}$ s. Since the time-constants are larger than the off time, the suppression factor becomes $\exp(-t_{off}/\tau_{leak})$. In this case the compensation between the CPDC mode and the MDFR mode does not occur, and the equation (6.41) is evaluated as;

$$\delta_{FRDC-DC} = \tau_{leak} \left(\frac{\tau'_{leak}}{\tau_{leak}} - \frac{\tau_{leak}}{\tau'_{leak}} \right) f_0 e^{-t_{off}/\tau_{leak}} = 2\alpha \cdot R_r \cdot R_{lc} \cdot f_0 \quad (6.42)$$

Hence a proportional increase of the FRDC-DC difference to the switching frequency f_{SW} is expected. The effect is also proportional to the input (load) resistance (R_r+R_{lc}). Using the specified circuit parameters, $R_r=1000\Omega$, $R_{lc}=25\Omega$ and $C_d=0.1$ pF, the (6.42) is evaluated as

$$\delta_{FRDC-DC} \approx 5.0 \times 10^{-11} f_{SW} \text{ (Hz)}. \quad (6.43)$$

The equation (6.43) is consistent with the measured value which is of the order of one ppm at the switching frequency of 10 kHz.

The linear dependence of FRDC-DC difference to switching frequency is also observed in the case of multijunction thermal converters. This phenomenon will be discussed in chapter 8.

6. 4 Summary

The significance of the FRDC method is that the thermoelectric transfer difference of a thermal converter can be evaluated experimentally. Otherwise, theoretical evaluation would

be the only way to evaluate the thermoelectric effects in thermal converters. The FRDC-DC difference measurement gives an independent method to cross-examine the theoretical evaluation.

A formula which characterizes the frequency-dependence of the FRDC-DC difference has been derived using a Fourier analysis, assuming a simple exponential behavior for the thermoelectric effects. The time constant of the thermoelectric effect of a thermal converter can be determined by the least-square fitting of the formula to FRDC-DC-difference data from the thermal converter.

The effect of shunt capacitance and the dielectric loss to the FRDC-DC difference has also been evaluated using the Fourier analysis. Due to the off-time inserted in the modified waveform, the effect is automatically compensated between the CPDC- and MDFR-modes. On the other hand, if the dielectric loss/absorption has characteristic time constant longer than the off-time, such compensation does not occur, and it can give rise to an additional FRDC-DC difference which is proportional to the switching frequency.